Gasification of waste biomass for hydrogen production: effects of pyrolysis parameters

Phuet Prasertcharoensuk[1], Steve J. Bull[1] and Anh N. Phan[1*]

[1]School of Engineering, Newcastle University, Newcastle Upon Tyne, UK.

*Corresponding authors: anh.phan@ncl.ac.uk

Abstract

Understanding the behaviour of pyrolysis is crucial in gasification of high volatile content lignocellulosic material. In this study, parameters affecting the properties of volatiles and char that are feedstock for the gasification step were studied to determine and optimize operating conditions in pyrolysis for high quality syngas/hydrogen production. A uniform temperature profile was obtained at particle sizes up to 0.5 cm^3. Pyrolysis temperatures in the range 600-900^oC significantly influence the char properties, i.e. increasing surface area and total pore size up to 2.5-3 times when increasing temperature, which in turn enhances the gas-solid reactions occurring in the gasification process. Increasing pyrolysis temperatures, i.e. above 700^oC fully decomposed unstable compounds, i.e. levoglucosan and their derivatives but promoted the formation of phenolic compounds. Around 41% reduction in surface area and total pore volume of the char was observed when increasing particle size from 0.5 to 2 cm^3. At pyrolysis temperatures above 800^oC and particle size of 0.5-1 cm^3 with a controlled amount of steam, i.e. 5.7 steam to carbon in biomass (S/C) molar ratio, the H_2 content in the gas phase increased to 67 mol% from 49 mol% and the aromatic compounds in the gas stream decreased up to 50.6%.

Keywords: waste wood, pyrolysis, gasification, hydrogen, particle size, temperature

1. Introduction

Among available renewable resources, only biomass contains the carbon and hydrogen that can be converted into fuels for the transportation sector and chemical production. Advanced thermochemical technologies, i.e. pyrolysis and gasification are considered as potential approaches to reduce the heavy dependency upon fossil fuels in the transportation sector (> 90% from fossil based fuels) and their associated environmental impacts. Direct conversion of biomass into liquid fuel via pyrolysis is still encountering a number of issues due to thermally and chemically unstable liquid products. However, biomass can be converted into gas via gasification that can be either used for transportation fuels, i.e. H_2 or converted further into hydrocarbons (via a Fischer-Tropsh synthetic route) or methanol. The concept of gasification of coal is well-known but there are issues when the same approach is applied to biomass. This is because biomass consists of 75-85% volatile matter as compared to only 20-35% in coal. Large amounts of volatiles in biomass are released rapidly in a very narrow temperature range (250-400^{o}C) [1, 2] potentially leading to the formation of high molecular weight compounds (known as tar) which are difficult to break down in later stages of processing and end up in the gas stream [3, 4]. Tar condenses at low temperatures (< 60^{o}C) causing operational difficulties for the downstream process (e.g. corrosion, clogging and fouling of installations) [4-6], requiring tar treatment/removal steps. In addition, some carbon and hydrogen content of the feedstock is lost, thus reducing the energy efficiency of the process. Therefore, fully understanding the effect of the pyrolysis on gasification stages is crucial to obtain high quality gas products in gasification process.

Extensive research has been done on the pyrolysis of lignocellulosic materials, focusing on the effects of operating conditions on yields and properties of the process e.g.

temperature [7-14], heating rate [15-19], vapour residence time [17, 20-23] and particle size of the feedstock [19, 22, 24-27]. However, these studies investigated pyrolysis as a single process without providing any links between the physicochemical properties of pyrolysis products and the operating parameters in the pyrolysis process that are required for syngas/hydrogen production via a gasification process. In this study, the effect of pyrolysis conditions on the gasification route in terms of quality of synthetic gas (syngas) and tar formation was investigated via two-stage gasification in which feedstock was decomposed into intermediate products and subsequently gasified, to provide an operating window for developing a simple, highly efficient and robust gasification unit that can be used for green hydrogen production without major downstream processing to remove impurities.

2. Materials and methods

2.1 Feedstock

Waste wood obtained from Sustainable Campus, Newcastle University was ground and sieved to 850 µm for characterisation (Figure 1a) and cut into cubes of 0.5 cm^3, 1 cm^3 and 2 cm^3 using a circular saw machine for experimental tests (Figure 1b). The waste wood had a very high volatile matter (84 wt%) and low ash content (< 1 wt%) compared to coal (20-35 wt% volatile and 10-20 wt% ash) as shown in Table 1. As a result, tighter controls are required in the oxidation step in the gasification process to ensure that all volatiles have a good contact time with the oxidising agent in order to get high quality gas and a char product which is highly reactive for solid-gas reactions occurring in a very short contact time (1-2 seconds) at high temperatures (> 800^{o}C), i.e. minimise the diffusion limitations to convert all the carbon content in the char into gas. Waste wood

had an empirical formula of $C_6H_{11}O_{5.5}N_{0.04}$ with 51 wt% oxygen content compared to around 7-10 wt% in coal.

(a) (b)

Figure 1: Examples of waste wood samples used for (a) characterisation and (b) pyrolysis experiments (1 cm^3 cube).

Table 1: Physicochemical characteristics of waste wood.

Proximate analysis (wt%, dry basis)	Values
Volatile matter	84.1 ± 0.4
Fixed carbon	15.4 ± 0.1
Ash content	0.5 ± 0.1
Ultimate analysis (wt%, dry basis, ash free)	Values
C	41.8 ± 0.3
H	6.4 ± 0.3
O*	51.5 ± 0.5
N	0.3 ± 0.3
HHV (MJ/kg)	17.7 ± 0.4
Empirical formula of waste wood	$C_6H_{11}O_{5.5}N_{0.04}$

*By difference

2.2 Experimental procedure

Approximately 25.0 ± 0.1 g of the waste wood (size 0.5, 1 or 2 cm^3) was placed in the centre of a 33 mm diameter and 830 mm long Inconel 600 fixed bed (Figure 2a). Prior to the experiments, the reactor was continuously purged with N_2. As soon as the system was air free (confirmed by gas chromatography), the N_2 was adjusted to a fixed flow rate of 30 or 120 ml/min to study the effect of vapour residence time (1-3 seconds) on product yields and properties in the pyrolysis step. The heating system was switched on at a fixed heating rate of 20^{o}C/min; it was found in preliminary trials in this study that there was no significant effect of the heating rate on product yields and characterisation of products between 5 and 20^{o}C/min. As soon as the set temperature reached, i.e. 600, 700, 800 or 900^{o}C, the system was held for a further 15 minutes before being switched off to ensure full decomposition of the volatiles released. The volatiles released from the pyrolysis were cooled down in two condensers, kept in an ice bath (0^{o}C), whereas the non-condensable gas was collected in a 500 ml tedlar sample bag for gas analysis. The solid residues and condensable liquid were collected and weighted for their yields and stored in glass bottles for further analysis when the reactor temperature was below 50^{o}C. The experimental set-up to examine the effect of pyrolysis product properties on the gasification stage is illustrated in Figure 2b. The volatiles released from the pyrolysis were passed through a char bed (which was produced by pyrolysis of waste wood at different temperatures of 600, 700, 800 or 900^{o}C as described previously) heated at 1000^{o}C. As soon as the volatiles from the pyrolysis stage were released (around 290-300^{o}C), steam was injected at the T-mixer before going into the gasification reactor at a steam to carbon in biomass (S/C) molar ratio of 5.7. The product collection and analysis procedure was the same as described previously in the pyrolysis step.

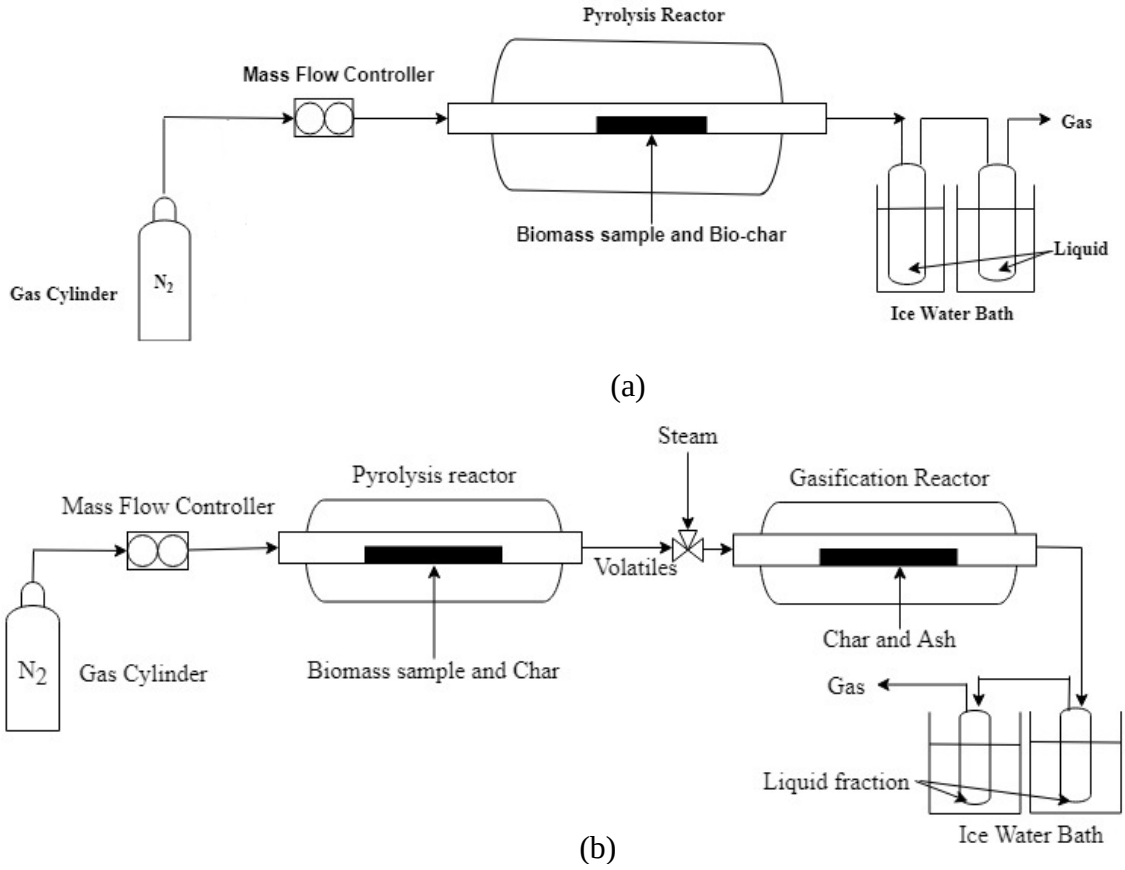

Figure 2: Schematic of (a) pyrolysis experiment and (b) two-stage gasification experiment.

2.3 Analysis

Solid residues (char) were tested for their proximate analysis including moisture content, volatile matter and ash content based on a British standard (BS-1016-6). The physical morphology of the waste wood sample before and after the pyrolysis was examined by a Hitachi TM 3030 Scanning Electron Microscope (SEM) operated at a 15 kV accelerating voltage. The specific surface area of char was determined from three random ground samples taken from a bulk sample by the Brunauer Emmett Teller (BET) nitrogen adsorption technique using a Thermo Scientific Surfer Gas Adsorption Porosimeter. There was considerable point to point variability in the samples due to the expected variability of the natural feedstock. The functional groups analysis of the char was carried

112 out using an Agilent Cary 630 FT-IR Spectrometer with scan range from 700 to 4000 cm^{-1}. The elemental analysis and the calorific value (HHV) of the char and condensed fraction (liquid) were carried out using an Elementar Vario MICRO Cube CHN Elemental Analyser and a CAL2K ECO Bomb calorimeter.

116 A Metrohm 827 pH meter was used to measure the pH of the liquid (bio-oil) at atmospheric temperature (20^{o}C). The water content in the liquid sample was measured using a Karl-Fischer titration (915 KF Ti-Touch), according to the American Society for Testing and Materials standard (ASTM E203-16). FT-IR analysis was carried out to characterize the organic functional groups in the liquid fraction using a ReactIR^{TM} 4000 FT-IR spectrometer, with scan range from 600-4000 cm^{-1}. The chemical compositions of the liquid samples were identified and quantified using a 7200 Accurate-Mass Q-TOF GC/MS and gas chromatography flame ionization detector (GC-FID) equipped with a 60 m x 250 µm x 0.25 µm capillary column (14%-cyanopropyl-phenly-methylpolysiloxane, Restek Rtx-1707) with helium as carrier gas.

126 Non-condensable gas was analysed using a Varian 450-GC gas chromatograph (GC) equipped with 5 columns and 3 detectors (1 TCD and 2 FID) with argon as carrier gas. A Molecularsieve ultimate 13X column (1.5 m × 1/8" × 2.0 mm) was used to detect the permanent gases (CO_2, CO, H_2, N_2 and CH_4). A Hayesep T and Q ultimetal column (0.5 m × 1/8" × 2.0 mm) was used to detect CO_2, C2s (acetylene, ethylene and ethane) and hydrocarbon gases. A CP-SIL 5CB capillary column (25 m × 0.25 mm × 0.4 µm) was used with a FID to determine hydrocarbons. A CP-WAX 52CB capillary column (25 m × 0.32 mm × 1.2 µm) equipped with another FID was used to detect light oxygenated compounds.

3. Results and discussion

3.1 Effect of pyrolysis temperature on product yields and properties

Table 2 shows that operating temperatures of 600-700^{o}C had little effect on product yields. A further increase in temperature to 700-800^{o}C resulted in a 23% increase in gas yield mainly at the expense of the liquid. This is because the devolatilization of the feedstock almost ceased at temperatures above 700^{o}C and volatiles were deeply cracked at high temperatures to form gases. This was evidenced by the amount of fixed carbon and the char carbon content remaining constant at 93-94 wt% and 87 wt% as shown in Table 3. Although there is a small amount of volatiles (around 3-4 wt%) present in the char, they could be tightly bonded or locked in stable structures and could not be released at the tested operating conditions. The carrier gas flow rate in the range of 30-120 ml/min (volatiles residence time around 1-3 seconds) had little effect on the product yields (Table 2). This could be because the residence time was insufficient to promote significant cracking of the volatiles. A small increase in the extent of cracking (around 4%) has been reported by others at lower temperatures, i.e. 550^{o}C [13, 17, 19, 23, 28].

Table 2: Pyrolysis product yields over various pyrolysis temperature and nitrogen flow rates at a fixed particle size of 1 cm^3.

Temperature (^{o}C)/ N_2 flow rate (ml/min)	Char (wt%)	Liquid (wt%)	Gas* (wt%)
600/30	25.1 ± 0.2	50.5 ± 0.3	24.4 ± 0.2
600/120	25.3 ± 0.1	51.1 ± 0.1	23.6 ± 0.3
700/30	23.7 ± 0.1	50.5 ± 0.1	25.8 ± 0.2
700/120	23.7 ± 0.2	50.7 ± 0.3	25.6 ± 0.2
800/30	22.5 ± 0.3	47.7 ± 0.2	29.8 ± 0.1
800/120	22.5 ± 0.2	47.6 ± 0.2	29.9 ± 0.2
900/30	22.0 ± 0.2	46.9 ± 0.1	31.1 ± 0.1

900/120	22.2 ± 0.2	47.4 ± 0.2	30.4 ± 0.1

*By difference

As observed in Figure 3, hydroxyl groups (OH) at ~3300 cm^{-1} and the aliphatic C-H stretching vibration at ~2900 cm^{-1} in the raw material (Figure 3a) disappeared at temperatures, i.e. 600^{o}C (Figure 3b), whereas other functional groups, i.e. C=O (stretching vibration at ~1700 cm^{-1}), aromatic C-C/C=C (vibration at ~1600 cm^{-1}), C-O (stretching(peak at ~1100 cm^{-1}) and the aromatic C-H (stretching vibration between 700 cm^{-1} and 900 cm^{-1}), decreased their intensities with increasing pyrolysis temperatures and completely disappeared at temperatures above 700^{o}C (Figure 3c-e). The results obtained from this study (Figure 3) agree very well with other findings [29-33], where functional groups on the char surface started to decrease at pyrolysis temperatures above 550^{o}C. Removal of functional groups at high temperatures provides char with high stability and degree of condensation on the char [34-38].

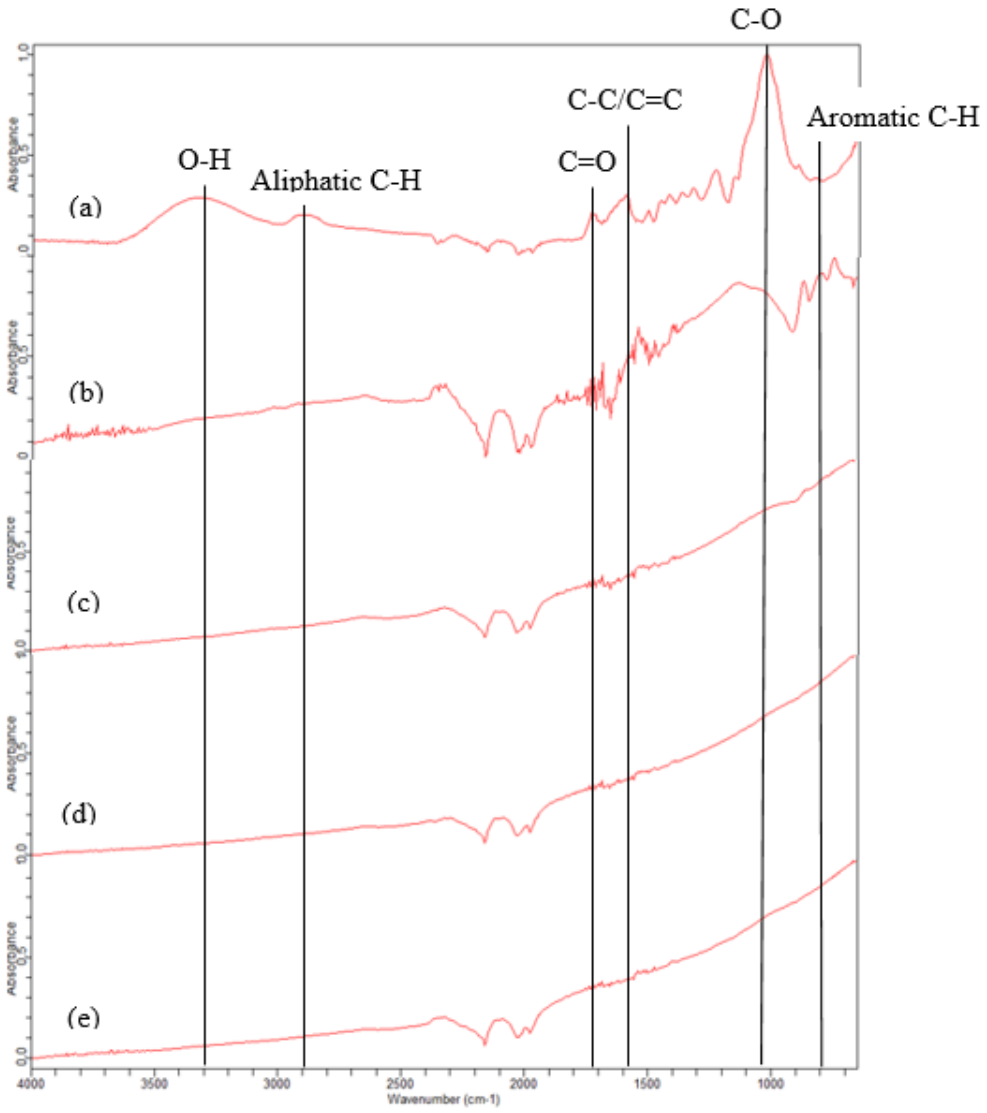

164 Figure 3: FT-IR spectra of (a) biomass feedstock (waste wood) and char obtained from
165 pyrolysis at a temperature of (b) 600°C; (c) 700°C; (d) 800°C and (e) 900°C at a fixed
166 nitrogen flow rate of 120 ml/min and particle size of 1 cm^3.

167 The experimental results (Table 3) showed that the energy content of the feedstock was
168 mainly stored in the liquid and char. The energy yield (which is defined as calorific value
169 of product*product yield/calorific value of raw material*mass of feedstock) was around
170 39-46% in char and 42-47% in liquid over the tested range of temperatures.

171 Table 3: Properties of pyrolysis products from pyrolysis of waste wood at 600 700, 800

172 and 900^{o}C at a fixed nitrogen flow rate of 120 ml/min and particle size of 1 cm^{3}.

Temperature (^{o}C)	600	700	800	900
Char properties (dry basis)				
Volatile matter (wt%)	10.1 ± 2.2	7.2 ± 1.7	4.6 ± 1.4	3.6 ± 1.9
Fixed carbon (wt%)	87.5 ± 1.3	90.2 ± 2.1	92.7 ± 1.0	93.6 ± 1.0
Ash content (wt%)	2.4 ± 1.1	2.6 ± 0.7	2.7 ± 0.7	2.8 ± 0.3
C ± 0.3 (wt%)	85.8	87.0	87.3	87.6
H ± 0.3 (wt%)	2.4	1.9	1.7	1.5
O ± 0.5* (wt%)	11.4	10.6	10.5	10.3
N ± 0.3 (wt%)	0.4	0.5	0.5	0.6
The empirical formula	$C_6H_2O_{0.6}N_{0.02}$	$C_6H_{1.6}O_{0.5}N_{0.03}$	$C_6H_{1.4}O_{0.5}N_{0.03}$	$C_6H_{1.2}O_{0.5}N_{0.04}$
HHV (MJ/kg)	32.5 ± 0.4	33.0 ± 0.1	33.5 ± 0.2	33.6 ± 0.4
BET surface area (m^2/g)	38.6 ± 1.7	78.9 ± 3.9	82.0 ± 4.2	98.4 ± 4.6
Liquid properties (wet basis)				
C ± 0.3 (wt%)	44.7	44.2	44.5	44.7
H ± 0.3 (wt%)	7.5	7.6	7.7	7.4
O ± 0.5* (wt%)	47.8	48.2	47.8	47.9
The empirical formula	$CH_2O_{0.8}$	$CH_{2.1}O_{0.8}$	$CH_{2.1}O_{0.8}$	$CH_2O_{0.8}$
Water content in liquid fraction (wt%)	43.9 ± 0.4	44.1 ± 0.8	44.6 ± 0.5	43.7 ± 0.8
pH	2.3 ± 0.2	2.3 ± 0.1	2.4 ± 0.2	2.4 ± 0.3
HHV (MJ/kg)	17.3 ± 0.4	16.5 ± 0.3	17.5 ± 0.4	17.2 ± 0.2
Gas composition				
H_2 (mol%)	12.5 ± 0.1	16.3 ± 0.3	18.3 ± 0.2	22.3 ± 0.3

CO (mol%)	38.5 ± 0.2	42.7 ± 0.1	45.4 ± 0.1	47.6 ± 0.2
CO_2 (mol%)	32.8 ± 0.1	27.5 ± 0.2	23.1 ± 0.1	15.1 ± 0.1
CH_4 (mol%)	9.6 ± 0.3	11.3 ± 0.1	11.7 ± 0.1	13.4 ± 0.2
C_2-C_5 (mol%)	6.6 ± 0.4	2.2 ± 0.2	1.5 ± 0.2	1.6 ± 0.2
H_2/CO	0.3	0.4	0.4	0.5

*By difference

Figure 4 shows the change in the char morphology with temperature. At a fixed particle size of 1 cm^3, increasing temperature accelerated the rate of decomposition [39-41], resulting in the formation of small pores on the surface of the char (where volatiles are released) from the smooth solid cells in the raw material (Figure 4a). The specific surface area of char increased from 38.6 m^2/g at 600ºC to 98.4 m^2/g at 900ºC (Table 3). A significant increase in the total pore volume from 21.7 × 10^{-3} cm^3/g to 52.1 × 10^{-3} cm^3/g and micropore (2-30 nm) volume from 13.1 × 10^{-3} cm^3/g to 34.4 × 10^{-3} cm^3/g was observed when increasing the pyrolysis temperature from 600 to 900ºC. The average pore diameter of the char surface was found to be in the range of 7-12 µm, suggesting a sufficient pore size to accommodate the volatiles from biomass, i.e. oxygenated compounds, heterocyclic aromatic and polycyclic aromatic hydrocarbons (PAHs) (< 2 µm) [42-44]. High total pore and micropore volumes will promote the mass transfer between gas and char particles, accelerating the heterogeneous solid-gas reactions, thereby reducing unburnt carbon in the ash residues [45, 46].

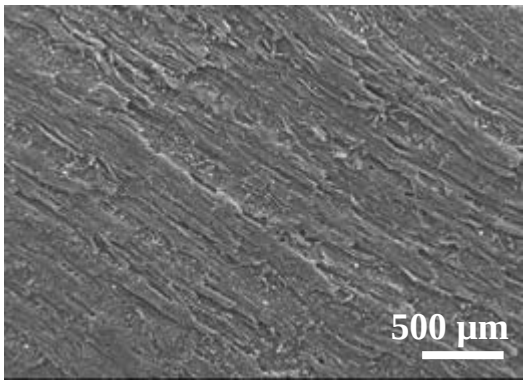

(a)

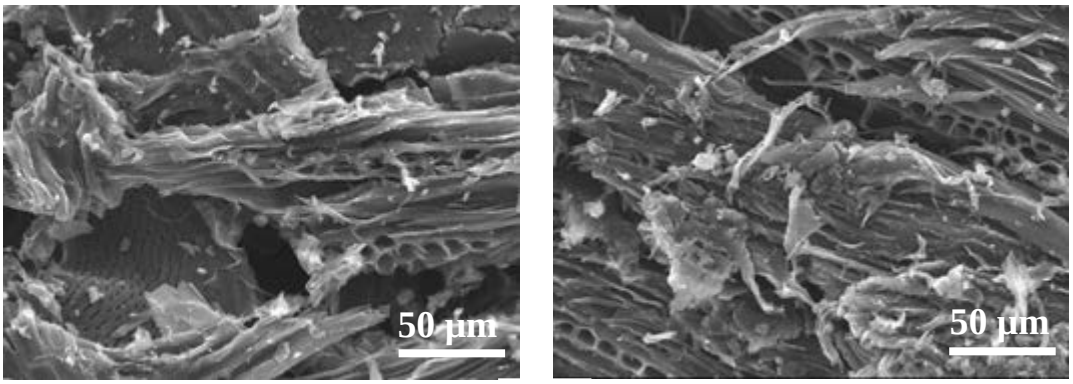

(b)

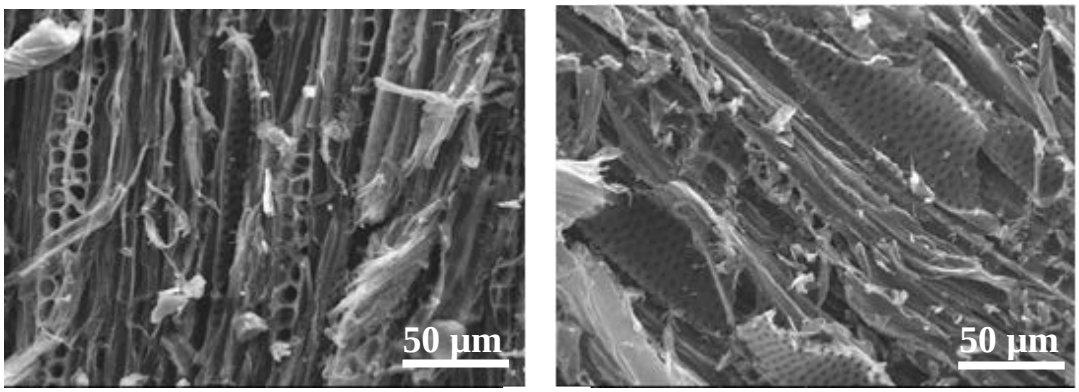

(c)

188 Figure 4: SEM images of (a) waste wood raw material (at a magnification of 38x) and
189 char (at a magnification of 500x) obtained from pyrolysis at a temperature of (b) 600^{o}C
190 and (c) 900^{o}C at a fixed nitrogen flow rate of 120 ml/min and particle size of 1 cm^{3}.

191 Table 3 shows the CO_2 concentration gradually decreased from 32.8 to 15.1 mol%,
192 whereas CO formation increased from 38.5 to 47.6 mol% when increasing pyrolysis
193 temperature from 600-900^{o}C. This is because when CO_2 was released from inner layers

of a particles it can react with a hot char layer via a Boudouard reaction ($C + CO_2 \rightarrow 2CO$), which is dominant at temperatures above 700°C, leading to the formation of CO [47]. Moreover, CO_2 could also react with other hydrocarbons (C_1-C_5) via a dry reforming reaction ($C_xH_y + xCO_2 \leftrightarrow 2xCO + \left(\frac{y}{2}\right)H_2$) to form H_2 and CO at temperatures above 640ºC [47, 48]. Although, the H_2/CO ratio increased when increasing temperature, i.e. from 0.3 at 600°C to 0.5 at 900°C due to an increase in H_2 and CO (Table 3), it is still much lower than the required ratios for syngas applications, i.e. chemical production and transportation fuel (H_2/CO > 1) [49-51].

The liquid product was highly acidic with pH of 2.3-2.4 containing a large amount of water (around 44 wt% (based on liquid fraction) or 22 wt% based on biomass feedstock (Table 3)). This causes the corrosion of installations and difficulties in ignition due to low calorific value, thereby reducing the local combustion temperature. The liquid product had much higher H/C and O/C ratios (H/C~2.0 and O/C~0.8) than heavy fossil-based oil (H/C~1.5 and almost zero oxygen) [52, 53]. If all water is removed, the liquid product would have a H/C in a range of 1.3-1.4 and O/C of 0.4-0.5, which is still higher than the required ratios for transport fuel applications. In addition, the liquid derived from pyrolysis is chemically unstable due to more than 300 chemical compounds, oxygen-containing compounds in particular (i.e. hydroxyacetaldehyde, 5-hydroxymethylfurfural, acetol, phenol and derivatives, levoglucosan and anhydrosugars) [54-56] that are present in the liquid product. As shown in Table 4 full decomposition of unstable compounds (i.e. sugars and their derivatives) was observed at pyrolysis temperature above 700°C, while the concentration of other compounds derived from decomposition of cellulose and hemicellulose, i.e. acids, ketones, aldehydes and furans gradually decreased with increasing temperature. However, phenol and its derivatives increased with temperature

due to Diels-Alder reactions which are favoured at high temperatures [57]. At all tested temperatures the liquid consisted mainly of furan and its derivatives and phenolic compounds (around 60% (Table 4)). This indicates that high temperature alone cannot decompose aromatics into gaseous products.

Table 4: Chemical compositions of liquid derived from pyrolysis of waste wood over various pyrolysis temperature at a fixed nitrogen flow rate of 120 ml/min and particle size of 1 cm^3.

Function groups	wt% (dry basis)			
	600°C	700°C	800°C	900°C
Acids	2.1	1.3	0.8	0.7
Esters	1.4	1.6	0.5	0.6
Ketones	2.9	2.6	0.9	1.0
Alcohols	1.1	1.1	0.8	0.7
Aldehydes	1.1	1.1	0.6	0.6
Furan and its derivatives	4.9	4.4	4.9	3.7
Sugars	1.5	0.3	-	-
Phenol and its derivatives	12.7	15.4	16.7	18.1
Unknown	1.0	0.6	1.1	1.3

3.2 Effect of particle size on product yields and properties

Decreasing particle size from 2 cm^3 to 0.5 cm^3 had a significant effect on the char and gas yields, i.e. an approximately 31% decrease in the char yield and 29% increase in the gas yield (Table 5). This is due to heat transfer limitation in larger particles, causing higher temperature gradients inside the particles. It took around 46 minutes for the middle of 0.5 cm^3 particle to reach the set temperature of 900°C but 52 minutes for 1 cm^3 and up to 62 minutes for 2 cm^3. The outer char layer could act as a hard shell hindering the release of volatiles [58, 59], resulting in increasing char yield from 19.8 wt% for 0.5 cm^3 to 28.7

wt% for 2 cm^3) and the volatile content remaining in char (6.5 wt% for 2 cm^3 but only 2.3 wt% for 0.5 cm^3) as shown in Table 5. Thus, understanding the temperature profile of single particles could help in designing a gasifier that provides sufficient time for decomposition of fuels. Although, there was little variation in C, H, O content (Table 5), the specific surface area of the char was significantly enhanced up to 124.5 m^2/g at 0.5 cm^3 compared to 73.0 m^2/g at 2 cm^3. The small variation in the repeated measurements (5%) was because different char samples derived from different waste wood feedstock pieces were chosen when determining specific surface area. As shown in Figure 5, the presence of cracking and development of the pore structure (micropores and macropores) was observed for the small particle size due to the rapid release of volatiles. Decreasing particle size from 2 cm^3 to 0.5 cm^3 led to increases in the total pore volume from 39.1 × 10^{-3} cm^3/g to 66.3 × 10^{-3} cm^3/g and the micropore volume from 23.1 × 10^{-3} cm^3/g to 42.9 × 10^{-3} cm^3/g.

Table 5: Product yields and properties obtained from pyrolysis of waste wood at different particle sizes 0.5, 1 and 2 cm^3 at pyrolysis temperature of 900ºC and nitrogen flow rate of 120 ml/min.

Particle size (cm^3)	0.5	1	2
Product yields			
Char (wt%)	19.8 ± 0.2	22.2 ± 0.2	28.7 ± 0.2
Liquid (wt%)	47.6 ± 0.2	47.4 ± 0.2	46.0 ± 0.2
Gas* (wt%)	32.6 ± 0.2	30.4 ± 0.1	25.3 ± 0.1
Char properties (dry basis)			
Volatile matter (wt%)	2.3 ± 1.0	3.6 ± 1.9	6.5 ± 1.4
Fixed carbon (wt%)	95.6 ± 2.2	93.6 ± 1.0	91.1 ± 1.9
Ash content (wt%)	2.1 ± 1.1	2.8 ± 0.3	2.4 ± 0.7

C ± 0.3 (wt%)	87.9	87.6	87.4
H ± 0.3 (wt%)	1.4	1.5	1.7
O ± 0.5* (wt%)	10.1	10.3	10.4
N ± 0.3 (wt%)	0.6	0.6	0.5
The empirical formula	$C_6H_{1.1}O_{0.5}N_{0.04}$	$C_6H_{1.2}O_{0.5}N_{0.04}$	$C_6H_{1.4}O_{0.5}N_{0.03}$
HHV (MJ/kg)	34.0 ± 0.4	33.6 ± 0.4	33.3 ± 0.5
BET surface area (m^2/g)	124.5 ± 5.3	98.4 ± 4.6	73.00 ± 3.2
Liquid properties (wet basis)			
C ± 0.3 (wt%)	46.4	44.7	41.5
H ± 0.3 (wt%)	7.4	7.4	7.1
O ± 0.5* (wt%)	46.2	47.9	51.4
The empirical formula	$CH_{1.9}O_{0.7}$	$CH_2O_{0.8}$	$CH_2O_{0.9}$
Water content in liquid fraction (wt%)	43.6 ± 0.4	43.7 ± 0.8	46.2 ± 0.4
pH	2.4 ± 0.2	2.4 ± 0.3	2.3 ± 0.3
HHV (MJ/kg)	18.0 ± 0.4	17.2 ± 0.2	14.9 ± 0.7
Gas composition			
H_2 (mol%)	24.4 ± 0.2	22.3 ± 0.3	18.2 ± 0.2
CO (mol%)	49.4 ± 0.3	47.6 ± 0.2	47.1 ± 0.3
CO_2 (mol%)	11.0 ± 0.1	15.1 ± 0.1	20.5 ± 0.2
CH_4 (mol%)	14.4 ± 0.3	13.4 ± 0.2	10.4 ± 0.2
C_2-C_5 (mol%)	0.8 ± 0.1	1.6 ± 0.2	3.8 ± 0.1
H_2/CO	0.5	0.5	0.4

*By difference

Due to the significant difference in temperature observed for large particles, an increase of CO_2 from 11.0 to 20.5 mol% and light hydrocarbon (C_2-C_5) from 0.8 to 3.8 mol% was observed, whereas other gas concentrations gradually decreased with increasing particle size from 0.5 cm^3 to 2 cm^3. As shown in Table 5, reducing particle size to 0.5 cm^3 had little effect on the ratio of H_2/CO (around 0.5).

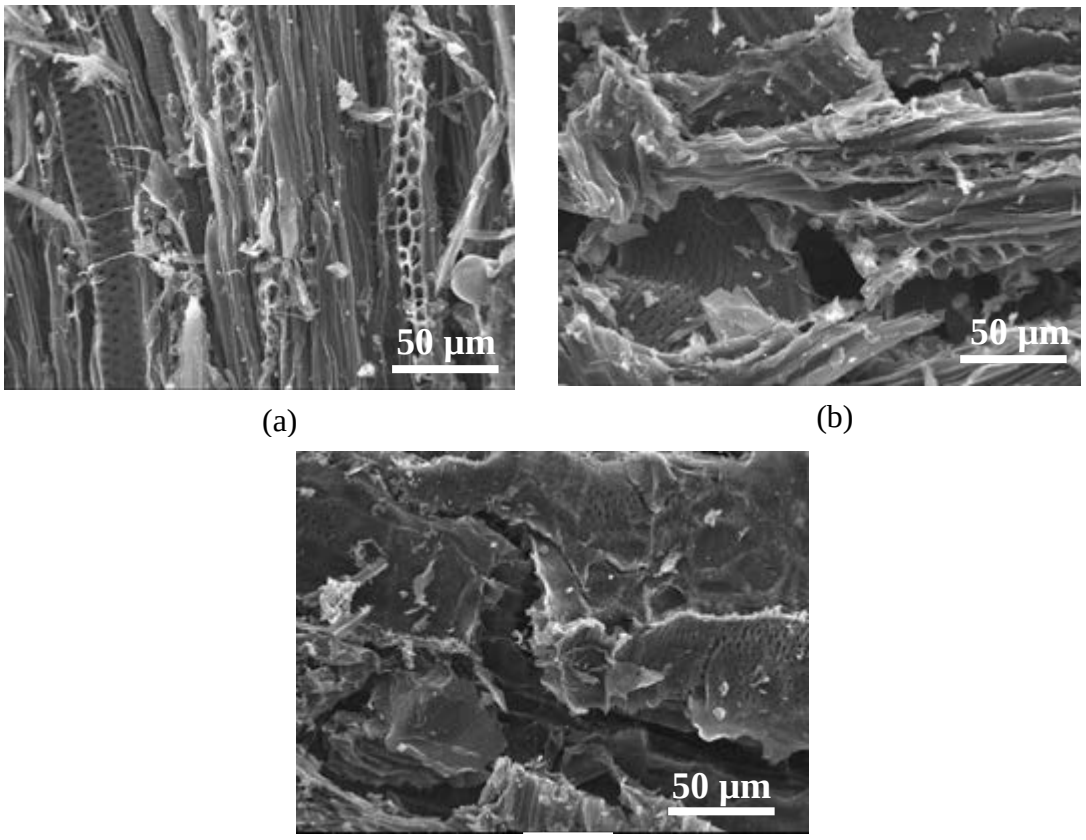

(a) (b)

(c)

Figure 5: SEM images at a magnification of 500x of char obtained from (a) 0.5 cm^3; (b) 1 cm^3 and (c) 2 cm^3 at pyrolysis temperature of 900ºC and nitrogen flow rate of 120 ml/min.

As illustrated in Table 5, increasing particle size slightly decreased the carbon content in the liquid (from 46.4 wt% for 0.5 cm^3 to 41.5 wt% for 2 cm^3) but the water content in liquid fraction increased slightly (around 6%). This could be due to the rapid release of volatile matter, minimising secondary reactions (i.e. dehydration) when small particles are used [13, 14, 60, 61]. The calorific values (HHV) of the liquid decreased from 18.0 MJ/kg at 0.5 cm^3 to 14.9 MJ/kg at 2 cm^3. Phenol and its derivatives decreased from 18.6 wt% at 0.5 cm^3 to 13.7 wt% at 2 cm^3 (Table 6). This could be due to an incomplete decomposition of lignin in the feedstock [56, 57, 62]. However, the concentration of other compounds gradually increased with increasing particle size as shown in Table 6.

Table 6: Compositions of liquid (condensable volatiles) derived from pyrolysis of waste wood over a range of particle sizes (0.5, 1 and 2 cm^3) at pyrolysis temperature of 900ºC and nitrogen flow rate of 120 ml/min.

Functional groups	wt% (dry basis)		
	0.5 cm^3	1 cm^3	2 cm^3
Acids	0.7	0.7	0.9
Esters	1.6	0.6	1.1
Ketones	0.8	1.0	2.2
Alcohols	1.0	0.7	1.3
Aldehydes	0.6	0.6	1.0
Furan and its derivative	2.8	3.7	4.3
Phenol and its derivatives	18.6	18.1	13.7
Unknown	0.8	1.3	0.3

3.3 The effect of pyrolysis conditions on gasification process

Pyrolysis products obtained from three different pyrolysis temperatures (i.e. 600, 800 and 900ºC) at a fixed particle size of 1 cm^3 and nitrogen flow rate of 120 ml/min were used to examine the effect of pyrolysis on the syngas quality and tar formation in two-stage gasification. Gasification was fixed at a temperature of 1000ºC and a steam to carbon in biomass (S/C) molar ratio of 5.7. Table 7 shows that the tar concentration in the gas stream significantly decreased from 42.9 g/Nm^3 (products derived at 600ºC pyrolysis) to 21.2 g/Nm^3 (products derived at 900ºC pyrolysis), corresponding to approximately 50.6% tar removal. This could be because the high specific surface area and pore volume of the char derived at high pyrolysis temperature (Table 3) promotes cracking/reforming of tars [63-66]. Moreover, the high porosity of char also enhances access of the gasifying agent (O_2, CO_2 or steam) to form H_2 and CO via the heterogeneous solid-gas reactions occurs in the gasification process, i.e. the Boudouard reaction ($C + CO_2 \rightarrow 2CO$) and the water

gas reaction ($C + H_2O \rightarrow 2CO + H_2$) [67-69]. The H_2 and CO in the syngas increased from 48.8 to 67.2 mol% and 4.5 to 8.8 mol% with the products derived at pyrolysis temperature of 600 and 900°C respectively (Table 7). Increasing the pyrolysis temperature from 600-900°C alters the gas yield (from 77.8 to 95.8 wt%) at the expense of solid residues (ash) (from 16.3 to 0.4 wt%) and unburnt carbon in the ash residues (< 0.01 wt%) at a fixed gasification temperature of 1000°C and a steam to carbon in biomass (S/C) molar ratio of 5.7 (Table 7). Moreover, an enhancement in the gas properties (higher CO concentration in the gas stream), which results in an increased pyrolysis temperature (Table 3), promotes a significant reaction, i.e. water gas shift reaction ($CO + H_2O \leftrightarrow CO_2 + H_2$), which occurs in the gasification step leading to the formation of H_2 in the gas stream.

Table 7: The effect of pyrolysis temperature on two-stage gasification at a fixed gasification temperature of 1000°C and a steam to carbon in biomass (S/C) molar ratio of 5.7.

Pyrolysis temperature (°C)	600	800	900
Gas yield (wt%)	77.8 ± 3.4	88.0 ± 2.1	95.8 ± 3.1
CO_2 (mol%)	39.0 ± 2.3	31.9 ± 1.2	21.8 ± 3.3
H_2 (mol%)	48.8 ± 1.3	56.8 ± 1.2	67.2 ± 1.4
CH_4 (mol%)	7.7 ± 0.7	4.7 ± 1.2	2.2 ± 1.2
CO (mol%)	4.5 ± 0.8	6.6 ± 1.1	8.8 ± 0.3
Tar (g/Nm^3)	42.9	34.7	21.2
Solid residues (wt%)	16.3 ± 1.4	7.3 ± 0.7	0.4 ± 1.1

Parameters affecting the pyrolysis process and the gas properties derived from gasification in this study can be applied for other high-volatile containing feedstock (75-85%). The initial waste wood composition (C, H, N, O) was found to have little influence on products derived from pyrolysis process [70-72]. However, the amount of steam

301 required for the gasification process should be adjusted according to the initial carbon
302 content in the feedstock to maintain the optimum ratio. Ash in lignocellulosic materials
303 contains mainly alkaline and other metals (Na, K, Si, Ca, Mg etc.) and remains as a solid
304 residue. These metals could act as catalysts for reforming/cracking of high molecular
305 weight compounds in both pyrolysis and gasification processes [64, 65], promoting less
306 tar formation. However, these inorganic species could cause a number of challenges such
307 as fouling, erosion and corrosion of installations as well as slagging and agglomeration
308 when the gasification temperature is above 1200^{o}C (melting point). The process
309 developed in this study is carried out at a temperature range of 1000-1100^{o}C, which only
310 just enough to transfer these metals into stable forms, i.e. NaO, Al_2O_3, P_2O_5, K_2O, K_2CO_3,
311 KCl, SiO_2, Fe_2O_3, $CaCO_3$, CaO and MgO [73, 74].

312 ## 4. Conclusions

313 The effects of pyrolysis temperature (600-900^{o}C), nitrogen flow rate (30 and 120 ml/min
314 corresponding to volatile residence time of 1-3 seconds) and particle size (0.5, 1 and 2
315 cm^3) on the product yields and properties of pyrolysis of waste wood were investigated.
316 Decreasing the particle size of the feedstock increased the specific surface area and total
317 pore volume of the char from 73.0 m^2/g and 39.1 × 10^{-3} cm^3/g at 2 cm^3 to 124.5 m^2/g and
318 66.3 × 10^{-3} cm^3/g at 0.5 cm^3. There were strong interactions between pyrolysis operating
319 conditions and the gasification step. Temperature in the pyrolysis process strongly altered
320 the char morphology (around 2-3 time increase in surface areas, total pore and micropore
321 volumes) and composition of the volatile products, which in turn had a strong influence
322 on the syngas properties, i.e. tar, carbon in ash (residues) and hydrogen content in
323 gasification. Increasing pyrolysis temperature increased hydrogen content whilst
324 decreasing hydrocarbons, CO_2 and tar content in the gas stream. Pyrolysis temperatures

above 700°C promoted the formation of phenolic compounds that would be precursors of multiple aromatic ring species in the gas products in gasification. Nonetheless, only decreasing size to 0.5 cm^3 and applying high temperature in pyrolysis would not be sufficient to produce high H_2/CO ratio (only 0.4-0.5). Our findings show that at a pyrolysis temperature of 900°C, a particle size of 0.5-1 cm^3 and at a controlled steam to carbon in biomass (S/C) molar ratio, i.e. 5.7, the H_2 content in gasification products increased up to 67 mol% from around 49% whereas the aromatic compounds decreased by up to 50.6%. The carbon content in ash (residues) from gasification was less than 0.01 wt%.

References

[1] Seo, D.K., S.S. Park, J. Hwang, and T.-U. Yu, Study of the pyrolysis of biomass using thermo-gravimetric analysis (TGA) and concentration measurements of the evolved species. Journal of Analytical and Applied Pyrolysis, 2010. **89**(1): p. 66-73.

[2] Soria-Verdugo, A., E. Goos, and N. García-Hernando, Effect of the number of TGA curves employed on the biomass pyrolysis kinetics results obtained using the Distributed Activation Energy Model. Fuel Processing Technology, 2015. **134**: p. 360-371.

[3] Arena, U., Process and technological aspects of municipal solid waste gasification. A review. Waste Management, 2012. **32**(4): p. 625-639.

[4] Li, C. and K. Suzuki, Tar property, analysis, reforming mechanism and model for biomass gasification—An overview. Renewable and Sustainable Energy Reviews, 2009. **13**(3): p. 594-604.

[5] Milne T., E.R.a.A., Biomass Gasifier "Tars": Their Nature, Formation and Conversion. 1998, National Renewable Energy Laboratory.

[6] Zhang, L., C. Xu, and P. Champagne, Overview of recent advances in thermo-chemical conversion of biomass. Energy Conversion and Management, 2010. **51**(5): p. 969-982.

[7] Yoshikawa, A.P.a.K., Influence of Pyrolysis Temperature on Rice Husk Char Characteristics and Its Tar Adsorption Capability. Energies, 2012. **5**: p. 4941-4951.

[8] Mazlan, M.A.F., Y. Uemura, N.B. Osman, and S. Yusup, Fast pyrolysis of hardwood residues using a fixed bed drop-type pyrolyzer. Energy Conversion and Management, 2015. **98**: p. 208-214.

[9] Yang, Z., A. Kumar, R.L. Huhnke, M. Buser, and S. Capareda, Pyrolysis of eastern redcedar: Distribution and characteristics of fast and slow pyrolysis products. Fuel, 2016. **166**: p. 157-165.

[10] Bordoloi, N., R. Narzari, D. Sut, R. Saikia, R.S. Chutia, and R. Kataki, Characterization of bio-oil and its sub-fractions from pyrolysis of Scenedesmus dimorphus. Renewable Energy, 2016. **98**: p. 245-253.

[11] Shaaban, A., S.-M. Se, N.M.M. Mitan, and M.F. Dimin, Characterization of Biochar Derived from Rubber Wood Sawdust through Slow Pyrolysis on Surface Porosities and Functional Groups. Procedia Engineering, 2013. **68**: p. 365-371.

[12] Akhtar, J. and N.A.S. Amin, A review on process conditions for optimum bio-oil yield in hydrothermal liquefaction of biomass. Renewable and Sustainable Energy Reviews, 2011. **15**(3): p. 1615-1624.

371 [13] Aysu, T. and M.M. Küçük, Biomass pyrolysis in a fixed-bed reactor: Effects of
372 pyrolysis parameters on product yields and characterization of products. Energy,
373 2014. **64**: p. 1002-1025.
374 [14] Tan, Y.L., A.Z. Abdullah, and B.H. Hameed, Fast pyrolysis of durian (Durio
375 zibethinus L) shell in a drop-type fixed bed reactor: Pyrolysis behavior and
376 product analyses. Bioresource Technology, 2017. **243**: p. 85-92.
377 [15] Chen, D., J. Zhou, and Q. Zhang, Effects of heating rate on slow pyrolysis behavior,
378 kinetic parameters and products properties of moso bamboo. Bioresource
379 Technology, 2014. **169**: p. 313-319.
380 [16] Chen, D., Y. Li, K. Cen, M. Luo, H. Li, and B. Lu, Pyrolysis polygeneration of poplar
381 wood: Effect of heating rate and pyrolysis temperature. Bioresource Technology,
382 2016. **218**: p. 780-788.
383 [17] Moralı, U., N. Yavuzel, and S. Şensöz, Pyrolysis of hornbeam (Carpinus betulus L.)
384 sawdust: Characterization of bio-oil and bio-char. Bioresource Technology, 2016.
385 **221**: p. 682-685.
386 [18] Yorgun, S. and D. Yıldız, Slow pyrolysis of paulownia wood: Effects of pyrolysis
387 parameters on product yields and bio-oil characterization. Journal of Analytical
388 and Applied Pyrolysis, 2015. **114**: p. 68-78.
389 [19] Varma, A.K. and P. Mondal, Pyrolysis of sugarcane bagasse in semi batch reactor:
390 Effects of process parameters on product yields and characterization of products.
391 Industrial Crops and Products, 2017. **95**: p. 704-717.
392 [20] Jourabchi, S.A., S. Gan, and H.K. Ng, Pyrolysis of Jatropha curcas pressed cake for
393 bio-oil production in a fixed-bed system. Energy Conversion and Management,
394 2014. **78**: p. 518-526.

[21] Ly, H.V., S.-S. Kim, J.H. Choi, H.C. Woo, and J. Kim, Fast pyrolysis of Saccharina japonica alga in a fixed-bed reactor for bio-oil production. Energy Conversion and Management, 2016. **122**: p. 526-534.

[22] Encinar, J.M., J.F. González, and J. González, Fixed-bed pyrolysis of Cynara cardunculus L. Product yields and compositions. Fuel Processing Technology, 2000. **68**(3): p. 209-222.

[23] Moralı, U. and S. Şensöz, Pyrolysis of hornbeam shell (Carpinus betulus L.) in a fixed bed reactor: Characterization of bio-oil and bio-char. Fuel, 2015. **150**: p. 672-678.

[24] Buah, W.K., A.M. Cunliffe, and P.T. Williams, Characterization of Products from the Pyrolysis of Municipal Solid Waste. Process Safety and Environmental Protection, 2007. **85**(5): p. 450-457.

[25] Shirley J. Duarte, J.L., Dario Alviso, and Juan C. Rolón, Effect of Temperature and Particle Size on the Yield of Bio-oil, Produced from Conventional Coconut Core Pyrolysis. International Journal of Chemical Engineering and Applications, 2016. **7**(2): p. 102-108.

[26] Şensöz, S., İ. Demiral, and H. Ferdi Gerçel, Olive bagasse (Olea europea L.) pyrolysis. Bioresource Technology, 2006. **97**(3): p. 429-436.

[27] Di Blasi, C., C. Branca, V. Lombardi, P. Ciappa, and C. Di Giacomo, Effects of Particle Size and Density on the Packed-Bed Pyrolysis of Wood. Energy & Fuels, 2013. **27**(11): p. 6781-6791.

[28] Gerçel, H.F., Production and characterization of pyrolysis liquids from sunflower-pressed bagasse. Bioresource Technology, 2002. **85**(2): p. 113-117.

418 [29] Kim, W.-K., T. Shim, Y.-S. Kim, S. Hyun, C. Ryu, Y.-K. Park, and J. Jung,
419 Characterization of cadmium removal from aqueous solution by biochar produced
420 from a giant Miscanthus at different pyrolytic temperatures. Bioresource
421 Technology, 2013. **138**: p. 266-270.
422 [30] Chen, W., S. Shi, T. Nguyen, M. Chen, and X. Zhou, Effect of Temperature on the
423 Evolution of Physical Structure and Chemical Properties of Bio-char Derived
424 from Co-pyrolysis of Lignin with High-Density Polyethylene. Vol. 11. 2016.
425 3923-3936.
426 [31] Elmay, Y., Y. Le Brech, L. Delmotte, A. Dufour, N. Brosse, and R. Gadiou,
427 Characterisation of Miscanthus pyrolysis by DRIFTs, UV Raman spectroscopy
428 and Mass Spectrometry. Vol. 113. 2015.
429 [32] Liu, W.-J., H. Jiang, and H.-Q. Yu, Development of Biochar-Based Functional
430 Materials: Toward a Sustainable Platform Carbon Material. Chemical Reviews,
431 2015. **115**(22): p. 12251-12285.
432 [33] Gai, X., H. Wang, J. Liu, L. Zhai, S. Liu, T. Ren, and H. Liu, Effects of Feedstock
433 and Pyrolysis Temperature on Biochar Adsorption of Ammonium and Nitrate.
434 PLoS ONE, 2014. **9**(12): p. e113888.
435 [34] Rafiq, M.K., R.T. Bachmann, M.T. Rafiq, Z. Shang, S. Joseph, and R. Long,
436 Influence of Pyrolysis Temperature on Physico-Chemical Properties of Corn
437 Stover (Zea mays L.) Biochar and Feasibility for Carbon Capture and Energy
438 Balance. PLoS ONE, 2016. **11**(6): p. e0156894.
439 [35] Enders, A., K. Hanley, T. Whitman, S. Joseph, and J. Lehmann, Characterization of
440 biochars to evaluate recalcitrance and agronomic performance. Bioresource
441 Technology, 2012. **114**: p. 644-653.

442 [36] Figueredo, N.A.d., L.M.d. Costa, L.C.A. Melo, E.A. Siebeneichlerd, and J. Tronto,
443 Characterization of biochars from different sources and evaluation of release of
444 nutrients and contaminants. Revista Ciência Agronômica, 2017. **48**: p. 3-403.
445 [37] Song, W. and M. Guo, Quality variations of poultry litter biochar generated at
446 different pyrolysis temperatures. Journal of Analytical and Applied Pyrolysis,
447 2012. **94**: p. 138-145.
448 [38] Jindo, K., H. Mizumoto, Y. Sawada, M. Sánchez-Monedero, and T. Sonoki, Physical
449 and chemical characterizations of biochars derived from different agricultural
450 residues. Vol. 11. 2014.
451 [39] Pradhan, D., R.K. Singh, H. Bendu, and R. Mund, Pyrolysis of Mahua seed
452 (Madhuca indica) – Production of biofuel and its characterization. Energy
453 Conversion and Management, 2016. **108**: p. 529-538.
454 [40] Ertaş, M. and M. Hakkı Alma, Pyrolysis of laurel (Laurus nobilis L.) extraction
455 residues in a fixed-bed reactor: Characterization of bio-oil and bio-char. Journal
456 of Analytical and Applied Pyrolysis, 2010. **88**(1): p. 22-29.
457 [41] Abdel-Fattah, T., M. E. Mahmoud, S. B. Ahmed, M. Huff, J. Lee, and S. Kumar,
458 Biochar from woody biomass for removing metal contaminants and carbon
459 sequestration. Vol. 22. 2014.
460 [42] Yang, H.-H., S.-M. Chien, M.-R. Chao, and C.-C. Lin, Particle size distribution of
461 polycyclic aromatic hydrocarbons in motorcycle exhaust emissions. Journal of
462 Hazardous Materials, 2005. **125**(1): p. 154-159.
463 [43] Wu, S.P., S. Tao, and W.X. Liu, Particle size distributions of polycyclic aromatic
464 hydrocarbons in rural and urban atmosphere of Tianjin, China. Chemosphere,
465 2006. **62**(3): p. 357-367.

[44] Ladji, R., N. Yassaa, C. Balducci, and A. Cecinato, Particle size distribution of n-alkanes and polycyclic aromatic hydrocarbons (PAHS) in urban and industrial aerosol of Algiers, Algeria. Environmental Science and Pollution Research, 2014. **21**(3): p. 1819-1832.

[45] Rehrah, D., R.R. Bansode, O. Hassan, and M. Ahmedna, Physico-chemical characterization of biochars from solid municipal waste for use in soil amendment. Journal of Analytical and Applied Pyrolysis, 2016. **118**: p. 42-53.

[46] Arenas, E. and F. Chejne, The effect of the activating agent and temperature on the porosity development of physically activated coal chars. Carbon, 2004. **42**(12): p. 2451-2455.

[47] Kwon, E.E., Y.J. Jeon, and H. Yi, New candidate for biofuel feedstock beyond terrestrial biomass for thermo-chemical process (pyrolysis/gasification) enhanced by carbon dioxide (CO2). Bioresource Technology, 2012. **123**: p. 673-677.

[48] Leal, A.M.M., D.A. Kulik, and G. Kosakowski, Computational methods for reactive transport modeling: A Gibbs energy minimization approach for multiphase equilibrium calculations. Advances in Water Resources, 2016. **88**: p. 231-240.

[49] Chaudhari, S.T., S.K. Bej, N.N. Bakhshi, and A.K. Dalai, Steam Gasification of Biomass-Derived Char for the Production of Carbon Monoxide-Rich Synthesis Gas. Energy & Fuels, 2001. **15**(3): p. 736-742.

[50] Torres, W., S.S. Pansare, and J.G. Goodwin, Hot Gas Removal of Tars, Ammonia, and Hydrogen Sulfide from Biomass Gasification Gas. Catalysis Reviews, 2007. **49**(4): p. 407-456.

[51] Yang, H., R. Yan, H. Chen, D.H. Lee, and C. Zheng, Characteristics of hemicellulose, cellulose and lignin pyrolysis. Fuel, 2007. **86**(12): p. 1781-1788.

[52] Zhang, L., R. Liu, R. Yin, and Y. Mei, Upgrading of bio-oil from biomass fast pyrolysis in China: A review. Renewable and Sustainable Energy Reviews, 2013. **24**: p. 66-72.

[53] Oasmaa, A. and S. Czernik, Fuel Oil Quality of Biomass Pyrolysis OilsState of the Art for the End Users. Energy & Fuels, 1999. **13**(4): p. 914-921.

[54] Oasmaa, A., E. Leppämäki, P. Koponen, J. Levander, and E. Tapola, Physical characterisation of biomass-based pyrolysis liquids Application of standard fuel oil analyses. 1997.

[55] Jani Lehto, A.O., Yrjö Solantausta, Matti Kytö, David Chiaramonti, Fuel oil quality and combustion of fast pyrolysis bio-oils. 2013.

[56] Alvarez, J., G. Lopez, M. Amutio, J. Bilbao, and M. Olazar, Bio-oil production from rice husk fast pyrolysis in a conical spouted bed reactor. Fuel, 2014. **128**: p. 162-169.

[57] Cypres, R., Aromatic hydrocarbons formation during coal pyrolysis. Fuel Processing Technology, 1987. **15**: p. 1-15.

[58] Bennadji, H., K. Smith, M.J. Serapiglia, and E.M. Fisher, Effect of Particle Size on Low-Temperature Pyrolysis of Woody Biomass. Energy & Fuels, 2014. **28**(12): p. 7527-7537.

[59] Hanson, S., J.W. Patrick, and A. Walker, The effect of coal particle size on pyrolysis and steam gasification. Fuel, 2002. **81**(5): p. 531-537.

[60] Bai, X., P. Johnston, S. Sadula, and R.C. Brown, Role of levoglucosan physiochemistry in cellulose pyrolysis. Journal of Analytical and Applied Pyrolysis, 2013. **99**: p. 58-65.

[61] Ronsse, F., S. van Hecke, D. Dickinson, and W. Prins, Production and characterization of slow pyrolysis biochar: influence of feedstock type and pyrolysis conditions. GCB Bioenergy, 2013. **5**(2): p. 104-115.

[62] Branca, C., P. Giudicianni, and C. Di Blasi, GC/MS Characterization of Liquids Generated from Low-Temperature Pyrolysis of Wood. Industrial & Engineering Chemistry Research, 2003. **42**(14): p. 3190-3202.

[63] Paethanom, A. and K. Yoshikawa, Influence of Pyrolysis Temperature on Rice Husk Char Characteristics and Its Tar Adsorption Capability. Energies, 2012. **5**(12): p. 4941.

[64] Shen, Y. and Y. Fu, Advances in in situ and ex situ tar reforming with biochar catalysts for clean energy production. Sustainable Energy & Fuels, 2018. **2**(2): p. 326-344.

[65] Liu, J., Y. He, X. Ma, G. Liu, Y. Yao, H. Liu, H. Chen, Y. Huang, C. Chen, and W. Wang, Catalytic Pyrolysis of Tar Model Compound with Various Bio-Char Catalysts to Recycle Char from Biomass Pyrolysis. Vol. 11. 2016. 3752-3768.

[66] Anis, S. and Z.A. Zainal, Tar reduction in biomass producer gas via mechanical, catalytic and thermal methods: A review. Renewable and Sustainable Energy Reviews, 2011. **15**(5): p. 2355-2377.

[67] Ren, S., H. Lei, L. Wang, Q. Bu, S. Chen, and J. Wu, Hydrocarbon and hydrogen-rich syngas production by biomass catalytic pyrolysis and bio-oil upgrading over biochar catalysts. RSC Advances, 2014. **4**(21): p. 10731-10737.

[68] Menéndez, J.A., A. Domínguez, Y. Fernández, and J.J. Pis, Evidence of Self-Gasification during the Microwave-Induced Pyrolysis of Coffee Hulls. Energy & Fuels, 2007. **21**(1): p. 373-378.

[69] Shen, Y., Chars as carbonaceous adsorbents/catalysts for tar elimination during biomass pyrolysis or gasification. Renewable and Sustainable Energy Reviews, 2015. **43**: p. 281-295.

[70] Fu, P., W. Yi, X. Bai, Z. Li, S. Hu, and J. Xiang, Effect of temperature on gas composition and char structural features of pyrolyzed agricultural residues. Bioresource Technology, 2011. **102**(17): p. 8211-8219.

[71] Luo, Z., S. Wang, Y. Liao, J. Zhou, Y. Gu, and K. Cen, Research on biomass fast pyrolysis for liquid fuel. Biomass and Bioenergy, 2004. **26**(5): p. 455-462.

[72] Xu, R., L. Ferrante, C. Briens, and F. Berruti, Flash pyrolysis of grape residues into biofuel in a bubbling fluid bed. Journal of Analytical and Applied Pyrolysis, 2009. **86**(1): p. 58-65.

[73] Benedetti, V., F. Patuzzi, and M. Baratieri, Characterization of char from biomass gasification and its similarities with activated carbon in adsorption applications. Applied Energy, **227**, 2018, 92-99.

[74] Vassilev, S.V., D. Baxter, L.K. Andersen, and C.G. Vassileva, An overview of the composition and application of biomass ash. Part 1. Phase–mineral and chemical composition and classification. Fuel, 2013. **105**: p. 40-76.